Nuclear Engineering and Technology 57 (2025) 103729

Contents lists available at ScienceDirect

Nuclear Engineering and Technology

journal homepage: www.elsevier.com/locate/net

Original Article

The effect of storage conditions and computer model simplification on the thermal state of the RBMK-1500M2 cask

Kęstutis Račkaitis [a,*], Povilas Poškas [a], Robertas Poškas [a], Hussam Jouhara [b]

[a] Nuclear Engineering Laboratory, Lithuanian Energy Institute, Breslaujos 3, LT-44403, Kaunas, Lithuania
[b] Heat Pipe and Thermal Management Research Group, College of Engineering, Design and Physical Sciences, Brunel University London, Uxbridge, UB8 3PH, UK

ARTICLE INFO

Keywords:
Spent nuclear fuel
Interim storage
CONSTOR RBMK-1500/M2 cask
Thermal analysis
Computer model simplifications

ABSTRACT

Interim storage of spent nuclear fuel is a very important part of the overall nuclear power generation cycle. At Ignalina NPP, spent nuclear fuel is stored in interim storage facilities in specially designed casks before being transferred to a geological repository. The internal structure of spent nuclear fuel casks and the processes involved are quite complex. Therefore, simplifying and optimizing simulations for evaluating decay heat removal from the cask is worthwhile. In this paper, the effect of computer model simplifications on the thermal characteristics of the CONSTOR RBMK-1500/M2 cask stored in building-type and open-type storage facilities is presented. The modeling was carried out using the ANSYS Fluent code. The analysis showed a substantial impact of solar insolation. Also, in the case of the homogenization of the SNF load in the basket, higher temperatures are obtained compared with the case when detailed modeling of the internal basket structure is performed. Hence, it was demonstrated that the homogenization model can be used in safety assessment as a conservative approach for the modeling of decay heat removal from the cask.

1. Introduction

In order to reduce CO_2 emissions, the global energy sector is gradually switching to renewable energy sources [1]. However, it is necessary to have other alternatives for the diversification of energy sources. In terms of CO_2 emissions, nuclear power plants are the most suitable, and in order to reduce the probability of any accidents at such power plants and their scale, new generation reactors and small modular reactors are being developed. In this way, old nuclear power plants that are still in operation will gradually be replaced by modern, safely operating power plants. However, there are many old nuclear power plants in the world, and they need to be safely decommissioned by taking care of the radioactive waste generated during their lifetime. The most dangerous long-lived radioactive waste (including spent nuclear fuel) is planned to be disposed of in deep geological repositories, i.e., at a depth of about 0.5 km underground. As the world's only deep geological repository in Finland is approaching the operation stage, and others are still in the research and design stages, spent nuclear fuel (SNF) is stored in interim storage facilities. In these storage facilities, in most cases, the SNF is stored in specially designed casks. The casks are of various types, e.g., concrete or metal, with a special design for their cooling or without cooling.

A fuel assembly, once used in the core of a reactor and now retrieved, emits substantial heat and remains highly radioactive. Consequently, it must initially be kept in a spent fuel pool for its radioactivity and heat to diminish—a process that lasts a minimum of 5 years. After retention in a water pool, the fuel is loaded into casks and transported to a dry storage facility, which utilizes inert gas or air for cooling to maintain normal operating conditions. Accident conditions also need to be assessed during fuel storage ([2,3]), but this is not the focus of this work.

The Ignalina Nuclear Power Plant (Ignalina NPP), which operated RBMK-1500 water-cooled graphite-moderated channel-type power reactors, is currently undergoing decommissioning. At the plant site, two interim dry storage facilities house over 21 000 fuel assemblies. These are kept in non-ventilated casks (CASTOR RBMK-1500 (cast iron), CONSTOR RBMK-1500 (metal-concrete) and CONSTOR RBMK-1500/M2 (metal-concrete)).

Extensive research has been conducted on storage in ventilated casks for various types of SNF (PWR, BWR, WWER) [4–8]. Also, important studies were performed in Refs. [9,10]. Li et al. [9] employed the STAR-CCM + code to model the temperature and flow patterns in the case of gas leakage from the storage cask. The study analyzed processes

* Corresponding author.
E-mail address: Kestutis.Rackaitis@lei.lt (K. Račkaitis).

https://doi.org/10.1016/j.net.2025.103729
Received 1 February 2025; Received in revised form 16 May 2025; Accepted 29 May 2025
Available online 29 May 2025

of canister depressurization and thermal response during a gas leakage. Meanwhile Abboud [10] created a thermo-chemical model which was used to simulate a wide range of sensitivity parameters for spent nuclear fuel.

The non-ventilated cask was examined in studies [11–22, etc.]. In Ref. [12], a TN24P cask was analyzed numerically with ANSYS Fluent. The results of the thermal analysis showed good agreement with experimental data. In Ref. [13], the authors applied STAR-CCM + to analyze the thermal performance of the same cask, suggesting a simplified analysis method. In Ref. [14], investigations were focused on an Orano TN-32B cask and equivalent trends were observed in the peak temperature of fuel cladding and the surrounding temperature, though their predictions (using codes COBRA-SFS and STAR-CCM+) slightly exceeded experimental measurements. In Ref. [15], a thermal analysis of CONSTOR RBMK-1500 and CASTOR RBMK-1500 casks (located at Ignalina Nuclear Power Plant) was conducted using the ALGOR code for normal interim SNF storage conditions (50 years). Since there are no operational geological disposal facilities, SNF dry container storage facilities are likely to have a longer service life than originally anticipated. Since most canister degradation mechanisms are temperature dependent, it is critical to develop tools and techniques for identifying canisters that are at risk of damage due to prolonged thermal exposure. In Refs. [16,18], thermal analyses were performed for the same CASTOR RBMK-1500 and CONSTOR RBMK-1500 casks loaded with SNF stored for an extended period of time i.e., up to 300 years. The results highlighted a significant temperature reduction in the first 50 years. Analysis in Ref. [20] showed that an analytical model can predict the internal temperature distribution inside the cask. The resulting data were compared with those obtained numerically using the finite volume method implemented in STAR-CCM+ and were in good agreement. Paper [19] introduced a thermo-mechanical assessment of a SNF cask. The aim of the study was to investigate the behavior of the cask under thermal loads, in particular the impact of the gaps between the basket and the cask body. The temperatures of the cask's elements were analyzed using the ABAQUS finite element code. The results confirmed that the thermal changes and stresses inside the cask are relatively small compared to the accepted safety limits. Nevertheless, there is a strong dependence on the geometry of the gaps. The paper [21] examined the effect of fire on the thermal behavior of a CASTOR cask in an open interim storage facility. Simulations were carried out using the ANSYS Fluent code. A local sensitivity analysis of the thermal parameters to temperature variations was also performed. The analysis showed that in the case of a fire, the maximum (peak) temperature increase in the fuel load was about 10 °C. In Ref. [22], a numerical simulation using ANSYS Fluent was conducted to assess how the simplifications applied to the model affected the distribution of the temperature within a CASTOR RBMK-1500 (non-ventilated, located in open storage). The study aimed to discover if it is possible to use a 2D homogenized model for the determination of the removal of heat from a SNF cask. The results showed that the model's estimations are on a more conservative side; nevertheless, the maximum value of the fuel cladding temperature that the model estimated was similar to the realistic temperature of the 3D model. However, the temperature profile of the 2D model did not reflect the reality.

The purpose of this study is to assess the impact of computer model simplifications and cask storage conditions on the temperature distribution in a metal-concrete CONSTOR RBMK-1500/M2 spent nuclear fuel Ignalina NPP cask. The analysis showed that the highest temperatures were obtained in the case of the homogenization of the SNF load in the basket, as opposed to the other case when detailed modeling of the internal basket structure was performed. Therefore, the homogenization model can be used in safety assessments as a conservative approach for the modeling of decay heat removal from the cask.

2. Methodology

2.1. CONSTOR RBMK-1500/M2 cask model

CONSTOR RBMK-1500/M2 spent nuclear fuel casks are stored at Ignalina NPP in a building-type storage facility, but in this paper, for comparison purposes, interim storage is analyzed for building-type and open-type facilities. The general picture of the metal-concrete non-ventilated CONSTOR RBMK-1500/M2 storage cask and the inner basket is presented in Fig. 1.

The metal-concrete body, the outer ring basket, the inner basket and the lid system are the main parts of the cask. One hundred eighty-two (182) SNF rod bundles (91 SNF assemblies cut in half) are loaded into two baskets: the inner basket and the outer ring basket.

Once assembled and loaded with SNF, the CONSTOR RBMK-1500/M2 storage cask may be divided into 3 parts: A) the cask body and lid system; B) the outer ring basket with 80 fuel rod bundles; and **C)** the inner basket with 102 fuel rod bundles. A 30° segment was selected for the 3D modeling due to the cylindrical geometry of the cask and a similar flow structure (Fig. 2).

Detailed list of components, together with their materials used in the modeling, is provided in Table 1.

Part A is made up entirely of solid material and Part B is an outer ring zone with homogenized tube bundles, so there are no major challenges in modelling them. The most challenging geometry is that of Part C, which is composed of various solid components surrounded by helium gas. This part needs to be carefully evaluated and reasonably simplified. Therefore, this paper focuses on the impact of simplifying Part C on the modelling results.

An additional field of interest was the impact of interim storage conditions. Casks may be stored in an open-type storage where outdoor solar insolation has a significant impact and in building-type storage where the surrounding is more moderate. For this purpose, four cases are considered, referred as Cases I, II, III and IV. For Cases I and II, open-type storage was investigated, and for Cases III and IV, building-type storage was investigated. For Cases I and III, the most simplified internal basket model is used. The inner basket with loaded SNF is homogenized and treated as a solid cylindrical body with several layers (C6, C7, C8, C9) (Fig. 3, left side). In the numerical modeling, the temperature-dependent effective heat conductivity of the inner basket as a homogenous zone (body) has been determined taking into account only conduction and radiation. Much more complex but closer to reality are Cases II and IV (Fig. 3, right side). It should be noted that in Fig. 3 only one fuel rod bundle is shown, embedded in the basket tube and presented as a cylindrical body. Other fuel rod bundles have been omitted to make the picture clearer. In Cases II and IV the SNF bundles in the inner basket are modeled as solid homogeneous cylindrical bodies consisting of three parts: an upper inactive zone (C3), an active zone (C4) and a lower inactive zone (C5) (Fig. 2C). The temperature-dependent effective heat conductivity of the basket tube as a homogenous zone (body) has been determined for each part, taking into account only conduction and radiation. In Cases II and IV, the partitions and the large holes in the side wall of the basket are taken into account.

The total decay heat in the cask is 12 kW: 6 kW in the outer ring basket and 6 kW in the inner basket. These are the maximum heat load values of the tube bundles. Hence, the modeling assumes the worst case conditions. The heat generated in the inner basket active zone (Fig. 2C4) is transferred to the other solid parts (C1, C3, C5) by thermal conduction and to the helium environment by thermal conduction and convection. The outer ring basket (B1) is made of aluminum, and fuel rod bundles are placed into the prepared holes. These fuel rod bundles are treated in the same way as in the case of the inner basket i.e., top inactive zone (B2), active zone (B3) and bottom inactive zone (B4). The effective conductivity of these parts is taken into account in the modeling. The heat generated in the active zones of the outer ring basket (B3) is transferred by thermal conduction to the other solid parts (B1, B2, B4).

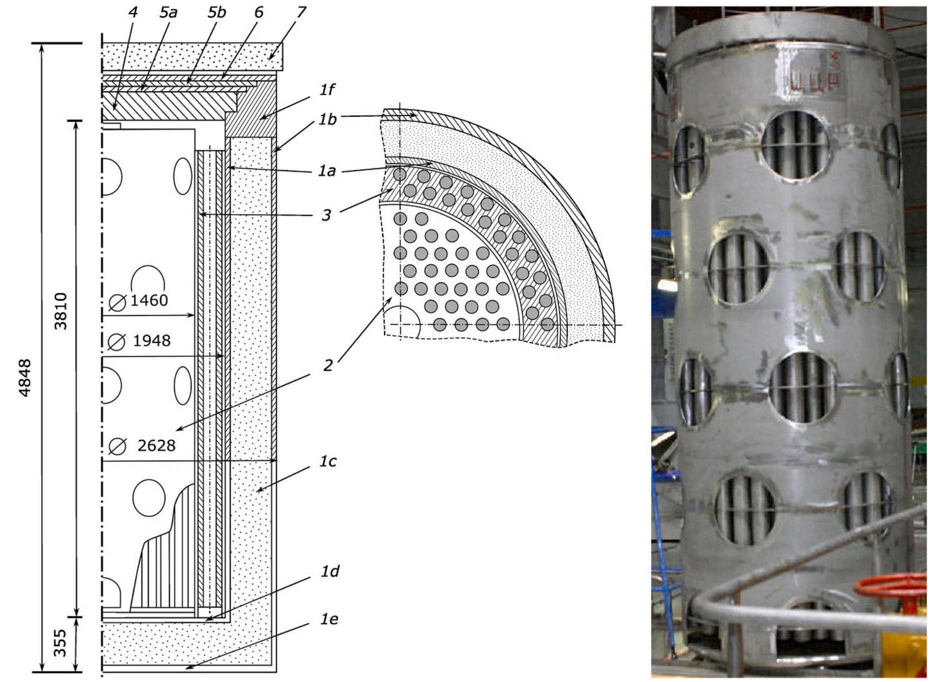

Fig. 1. Mockup of CONSTOR RBMK-1500-M2 storage cask (not to scale) (a) and photo of its inner basket (b): 1a) inner liner; 1b) outer liner; 1c) heavy concrete; 1d) inner liner bottom; 1e) outer liner bottom; 1f) cover ring; 2) the inner basket; 3) the outer ring basket; 4) the cask lid; 5) the steel sealing plates (5a, 5b); 6) the guard plate; 7) the concrete cover.

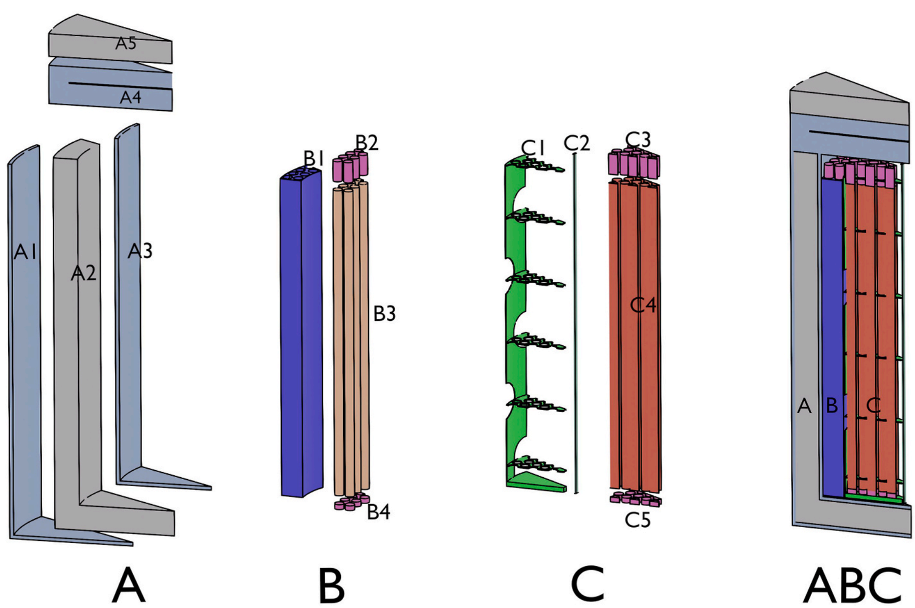

Fig. 2. Main components of CONSTOR RBMK1500/M2 cask 30° segment used in the modelling. A) the cask body; B) the outer ring basket with SNF; C) the inner basket with SNF. ABC shows all parts assembled together.

All the heat generated in the baskets is transferred by conduction through the cylindrical wall of the cask and by convection and thermal radiation through the helium gaps (adjacent to this wall). The sealing and baffle plates are modeled with an air gap (Fig. 2 A4). This gap is assumed to be a solid body, which means that only thermal conductivity is conservatively considered. Part (A) encloses parts (B) and (C) to form a sealed container. Heat is dissipated from the cask's outer surface to the environment through convection and thermal radiation resulting from a buoyancy-driven air flow. The thermal radiation will be evaluated taking into account the external horizontal concrete plate on the top of the cask. The thermal radiation has not been evaluated for the external vertical surface because the modeled container is located next to other containers in the interim storage facilities with similar wall temperatures. The convective heat flux has been estimated and included in the modeling as a heat transfer coefficient of 5 W/m^2K. This value is reasonable as the temperature of the external surfaces of the cask is relatively low, which leads to laminar air flow.

To assess the safety of SNF storage in a cask, critical conditions need to be investigated. One common critical condition is summer and peak solar radiation during the day. This paper in one part (Cases I and III) examines an open storage cask under extreme summer conditions. Simulations are performed under steady-state conditions. The boundary

Table 1
List of CONSTOR RBMK-1500/M2 cask components.

Label	Component name	Material
A1	Outer liner	steel
A2	Shielding material	concrete
A3	Inner liner	steel
A4	Seal and shim plates with effective air gap	steel
A5	Concrete plate	concrete
B1	Ring basket	aluminum
B2	Inactive zone at the top of fuel rod bundles	homogenized zone
B3	Active zone of the fuel bundle	homogenized zone
B4	Inactive zone at the bottom of rod fuel bundles	homogenized zone
C1	Basket 32M	steel
C2	Basket central tube	steel
C3	Inactive zone at the top of the fuel bundle	homogenized zone (Cases II and IV)
C4	Active zone of the fuel bundle	homogenized zone (Cases II and IV)
C5	Inactive zone at the bottom of the fuel bundle	homogenized zone (Cases II and IV)
C6	Inactive zone at the top of the inner basket	homogenized zone (Cases I and III)
C7	Active zone of the inner basket	homogenized zone (Cases I and III)
C8	Inactive zone at the bottom of the inner basket	homogenized zone (Cases I and III)
C9	Basket bottom	steel

conditions were set as follows: the ambient temperature was 37 °C and the cask was exposed to solar radiation. The value of 37 °C is based on the fact that this temperature was reached in 1994 and is the highest temperature ever reached in Lithuania. Due to the conservative approach, no account has been taken of the temperature drop at night.

The solar insolation values used were 100 W/m^2 for the cask's vertical surface and 400 W/m^2 for the horizontal surface. These values are half the values recommended by Ref. [23] for a 12-h day. Due to the high mass of the loaded cask, the temperature change in the cask is too slow for the day-night change to make a significant difference, and it is therefore possible to simplify the simulations. This method is consistent with conservative conditions for the following reasons: (a) the variation in day and night temperatures does not have a significant effect on the highest temperature of the cask; (b) the amount of heat generated by solar insolation over a 24-h day is the same as the recommended value over a 12-h day and a 12-h night; and (c) the value of the heat flux for the vertical surface is lower for an actual storage site, because the adjacent casks are placed at intervals of 3 m and are partly shadowed by other casks. Naturally, the external surface of the bottom of the cask is not taken into account for solar flux.

In the second part (Cases II and IV) the SNF cask was investigated at the real storage conditions in the building-type storage facility. The ambient temperature of the room in which the cask is stored is assumed to be the same as in the previous case, i.e., 37 °C. Only on the upper horizontal surface of the cask, it is assumed that the exhaust air will warm up to 50 °C. The bottom surface of the cask is assumed to be adiabatic.

The cask model was created with ANSYS SpaceClaim. The mesh was produced with the ANSYS Meshing tool and the calculations were performed using the ANSYS Fluent code. 3D steady-state Navier-Stokes equations for a laminar flow (Cases II and IV) with variable physical properties were used to perform the investigation. The radiation was solved using the Discrete Ordinates (DO) method [24] implemented in ANSYS Fluent.

For all cases a mesh validation was performed. Table 2 shows mesh validation results. Every case was tested with coarse, normal and fine meshes. Peak temperature differences between solutions with coarse and normal meshes were small compared to the required accuracy. The temperature differences between solutions with normal and fine meshes were negligible. Therefore results obtained with fine meshes are presented below.

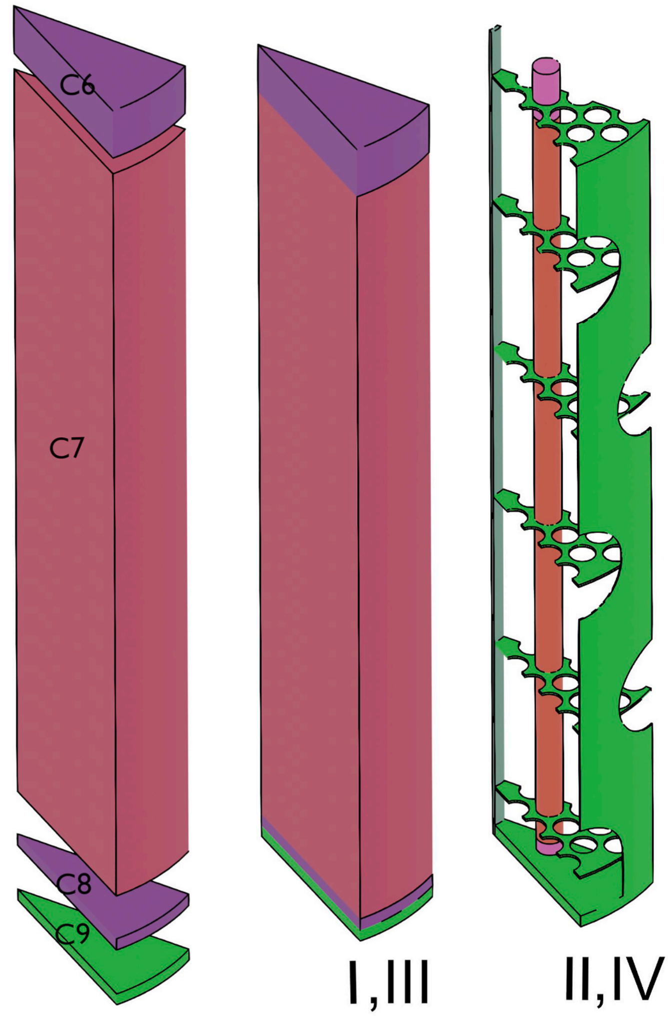

Fig. 3. Visualization of inner basket simplification for Cases I, III and II, IV.

Table 2
Mesh validation results for the peak temperatures in cases I-IV.

Case	Storage type	Description	Mesh	Cells	Peak temperature, °C
I	Open-type	Inner basket is homogenized	coarse	33 825 964	287.671
			normal	58 430 903	287.798
			fine	86 388 505	288.031
II	Open-type	Detailed inner basket	coarse	49 917 387	267.114
			normal	89 633 454	268.561
			fine	133 190 977	268.713
III	Building-type	Inner basket is homogenized	coarse	33 825 964	273.268
			normal	58 430 903	273.424
			fine	86 388 505	273.646
IV	Building-type	Detailed inner basket	coarse	49 917 387	248.732
			normal	89 633 454	249.609
			fine	133 190 977	249.808

3. Results

The numerical modeling at steady-state conditions shows different temperature distributions and values achieved (Fig. 4). A rather symmetrical temperature distribution is obtained for Cases I and III, where

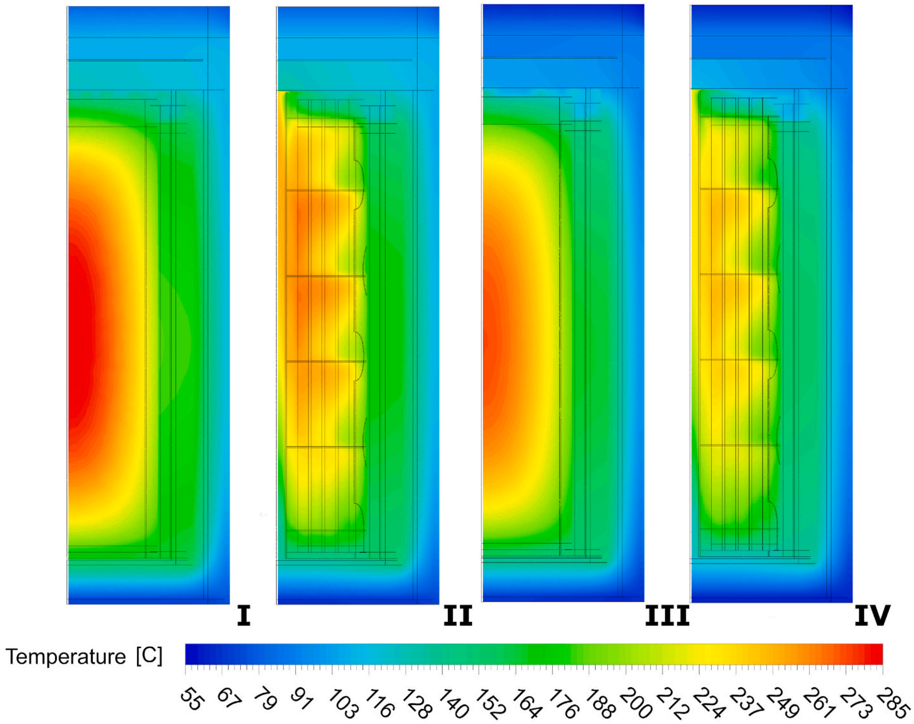

Fig. 4. Temperature (°C) distribution on a vertical symmetry plane for Cases I, II, III and IV.

the volume of the inner basket is modeled as a solid body. The hottest temperature value is on the axis of the cask at a height of 2.1 m above the ground. From this point, the temperature gradually decreases in both axial and radial directions (see also Fig. 5 for radial distribution).

The temperature distribution is different for Cases II and IV, where due to the internal structure, such as the central basket tube and the horizontal basket plates, and the free flow of helium and heat dissipation from the basket tubes, the hottest temperatures are shifted away from the center to the height of 2.5 m from the bottom (see also Fig. 5 for radial distribution).

As it is clear from Fig. 6, there is a quite similar helium flow structure in the cask regardless of its storage conditions (outside or inside storage facility). The highest velocities for both cases are achieved at the top of the central basket tube. Helium rises up though the central basket tube from the bottom and then falls back down in the narrow gap between the ring and the inner baskets. Helium from the upper partitions of the inner basket may mix with the lower partitions and return through the central part of the basket to close the loop.

Fig. 7 shows the fuel bundle location in the cask, and Fig. 8 demonstrates temperature behaviors. The highest temperatures in the cask are in the parts where most of the heat is generated. In Cases I and III, this is the axis of the cask, while in Cases II and IV this is the axis of the basket tubes.

The outer ring basket is a rather good medium for heat transfer because it is made of aluminum. It is closer to the outer surface of the cask, which helps to better remove decay heat in the radial direction.

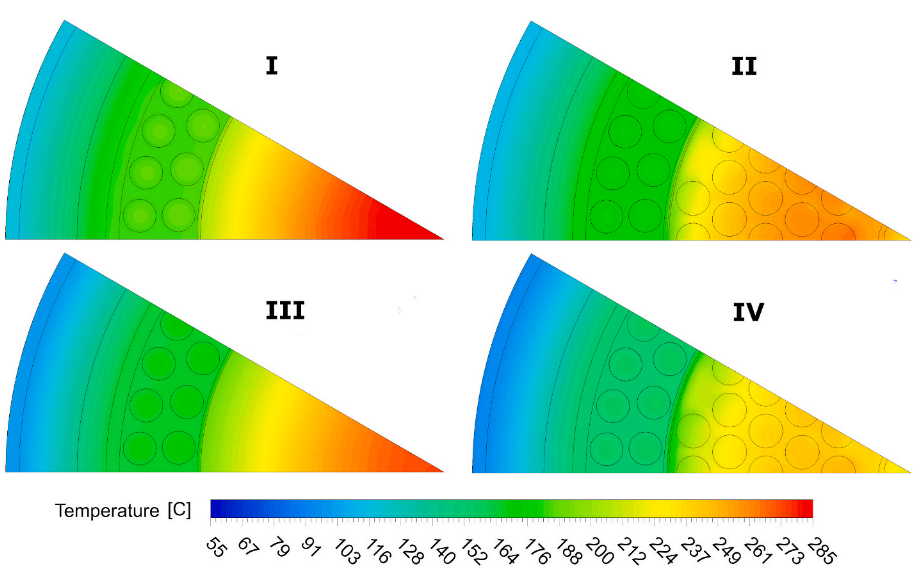

Fig. 5. Radial temperature distribution at the height of hottest temperature (For Cases I and III this height is at 2.1 m and for Cases II and IV this height is at 2.5 m level, measured from the bottom).

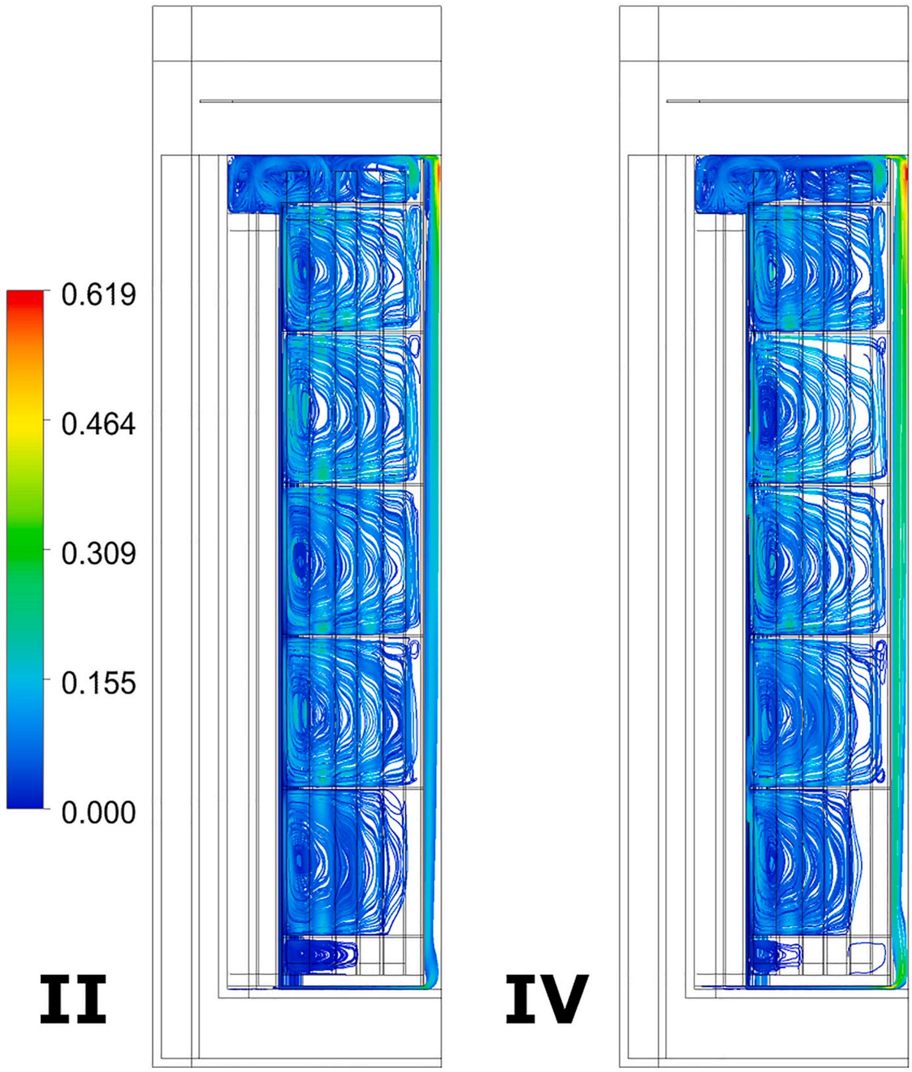

Fig. 6. Streamlines colored by velocity magnitude for Cases II and IV.

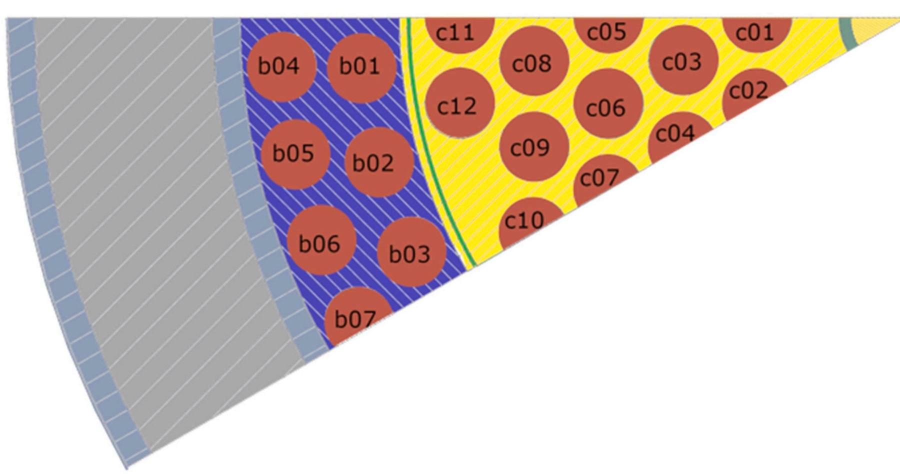

Fig. 7. Labels for the basket and ring basket tubes.

Aluminum is highly conductive and therefore provides good heat transfer in the axial direction.

As can be seen from Fig. 7a and b, the fuel rod bundle temperature variation in the outer ring basket is about 20 °C. The maximum temperature is observed at a height of 2.1 m from the bottom in Cases I and III and at 2.5 m height from the bottom in Cases II and IV. The outer ring basket has two groups of bundles, one closer to the cask's central axis and the other closer to the outer surface. The temperatures of fuel

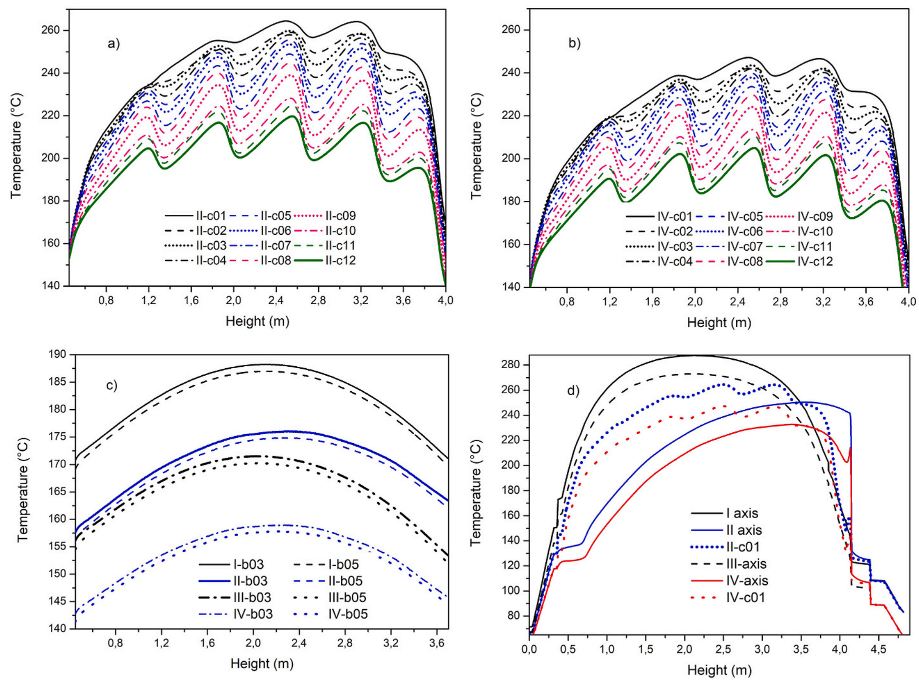

Fig. 8. Temperature distribution: a) Case II axes of the inner basket tubes; b) Case IV axes of the inner basket tubes; c) Cases I, II, III and IV axes of the outer ring basket tubes b03 and b05; d) Cases I, II, III and IV cask axes and Cases II, IV basket tube C01 axis.

rod bundles belonging to the same group are the same due to the good aluminum conductivity and symmetry to the cask axis. The temperature differs only if the bundle is placed at a different radius from the cask's central axis. However, this difference is less than 2 °C.

Greater temperature variations were observed for the inner basket. Fig. 7c, d shows temperature distributions in every basket tube for Cases II and IV respectively. The highest temperatures are in tube c01 axis in both cases. In Case I the highest temperature occurs on cask axis. Fig. 7d shows the cask axis temperature for all Cases and temperature of the hottest inner basket tube c01 for Cases II and IV. This figure shows that Cases I and II are the most conservative in calculations as the temperatures reached are ~40 °C higher than for more realistic Cases II and IV.

4. Conclusions

Four cases have been considered in this paper in an investigation of the effect of simplifying the computer model and storage conditions of the CONSTOR RBMK/M2 cask, when considering the highest temperatures and their distribution inside the cask. In Cases I and III the most simplified inner basket model was used. The inner basket with loaded SNF is homogenized and modeled as a solid cylindrical body. Much more complex, but closer to reality, were Cases II and IV. In these Cases, only SNF bundles in the inner basket and the outer ring basket tubes were modeled as homogenized solid cylindrical bodies. In all four Cases, the inner structure of the basket including the partitions and the large holes in the basket's side wall were taken into account. Cases I and II are for the open-type storage facility, and Cases III and IV are for the building-type storage facility. The results obtained during the investigation allow the following conclusions to be drawn:

1. When the inner basket was modeled as a homogenized solid body (Cases I, III), the highest temperatures were on the central axis of the cask, and they were about 20 °C higher than for the detailed modeling in Cases II and IV. The hottest temperature was obtained in the middle of the cask (at 2.1 m from the bottom).
2. Modeling results of Cases II and IV show that there is a clear circulation of the flow between partitions. The highest temperatures were shifted upwards to 2.5 m above the bottom, and they were smaller in comparison to Case I or Case III. The basket tube that was closest to the center of the cask had the highest temperature.
3. Comparison of Cases I and III or Cases II and IV shows that the effect of the storage facility's type may be evaluated. The results clearly showed that in the case of the building-type interim storage facility, the highest temperature of the fuel load was about 20 °C smaller than in the case of the open-type interim storage facility.

CRediT authorship contribution statement

Kęstutis Račkaitis: Writing – original draft, Methodology, Investigation. **Povilas Poškas:** Writing – review & editing, Methodology, Conceptualization. **Robertas Poškas:** Writing – review & editing, Resources. **Hussam Jouhara:** Writing – review & editing, Formal analysis.

Declaration of competing interest

The authors declare that they have no known competing financial interests or personal relationships that could have appeared to influence the work reported in this paper.

References

[1] A.G. Olabi, et al., Renewable energy systems: comparisons, challenges and barriers, sustainability indicators, and the contribution to UN sustainable development goals, Int. J. Thermofluids 20 (2023) 100498, https://doi.org/10.1016/j.ijft.2023.100498.

[2] S. Kim, S.S. Cho, Seismic analysis of free-standing spent-fuel dry storage cask considering soil–concrete pad–cask interaction, Nucl. Eng. Technol. 56 (2024) 4446–4454, https://doi.org/10.1016/j.net.2024.06.006.

[3] S. Alyokhina, Thermal analysis of certain accident conditions of dry spent nuclear fuel storage, Nucl. Eng. Technol. 50 (2008) 717–723, https://doi.org/10.1016/j.net.2018.03.002.

[4] Y.S. Tseng, J.R. Wang, F.P. Tsai, Y.H. Cheng, C. Shih, Thermal design investigation of a new tube-type dry-storage system through CFD simulations, Ann. Nucl. Energy 38 (2011) 1088–1097, https://doi.org/10.1016/j.anucene.2011.01.001.

[5] J. Li, Y.Y. Liu, Thermal modeling of a vertical dry storage cask for used nuclear fuel, Nucl. Eng. Des. 301 (2016) 74–88, https://doi.org/10.1016/j.nucengdes.2016.01.008.

[6] Y. Wu, J. Klein, H. Zhou, L. Zuo, Thermal and fluid analysis of dry cask storage containers over multiple years of service, Ann. Nucl. Energy 112 (2018) 132–142, https://doi.org/10.1016/j.anucene.2017.10.013.

[7] R. Ratiko, R. Sumarbagiono, A. Aisyah, W. Wati, K. Heriyanto, M. Mirawaty, P. A. Artiani, Y. Purwanto, D.L.I. Saputra, J. Rachmadetin, R. Setiawan, A. Istavara, A. A. Rauf, Theoretical and experimental analysis on influence of natural airflow on spent fuel heat removal in dry cask storage, Sustainability (Basel) 14 (2022) 1859, https://doi.org/10.3390/su14031859.

[8] M. Angelucci, S. Paci, F. Feria, L.E. Herranz, Uncertainty and sensitivity analysis of a dry cask for spent nuclear fuel, Energies 15 (2022) 1216, https://doi.org/10.3390/en15031216.

[9] J. Li, Z. Han, Y. Liu, H. Takeda, Using temperature and flow fields to detect gas leakage from canisters containing spent nuclear fuel: applications to RAMM-TM, Nucl. Eng. Des. 412 (2023) 112449, https://doi.org/10.1016/j.nucengdes.2023.112449.

[10] A.W. Abboud, Coupled chemical–CFD modeling of unsealed dry storage of advanced test reactor spent fuel, Ann. Nucl. Energy 183 (2023) 109646, https://doi.org/10.1016/j.anucene.2022.109646.

[11] J.M. Creer, T.E. Michener, M.A. McKinnon, J.E. Tanner, E.R. Gilbert, D. A. Dziadosz, M.F. Jensen, The TN-24P PWR spent-fuel storage cask: testing and analyses: interim report. Pacific Northwest Lab, Tech. rep., 1987.

[12] S.H. Yoo, H.C. No, H.M. Kim, E.H. Lee, Full-scope simulation of a dry storage cask using computational fluid dynamics, Nucl. Eng. Des. 240 (2010) 4111–4122, https://doi.org/10.1016/j.nucengdes.2010.08.009.

[13] R.A. Brewster, E. Baglietto, E. Volpenhein, C.S. Bajwa, CFD analyses of the TN-24p PWR spent fuel storage cask, Pres. Ves. Pip. Conf. 55027 (2012) 17–25.

[14] J.A. Fort, D.J. Richmond, J.M. Cuta, S.R. Suffield, Thermal Modeling of theTN-32B Cask for the High Burnup Spent Fuel Data Project, 2019, p. 94.

[15] P. Poškas, A. Šmaižys, V. Šimonis, Radiological and thermal characteristics of CASTOR RBMK-1500 and CONSTOR RBMK-1500 casks for spent nuclear fuel storage at Ignalina Nuclear Power Plant, Kerntechnik (1987) 71 (2006) 222–227, https://doi.org/10.3139/124.100297.

[16] R. Poškas, V. Šimonis, P. Poškas, A. Sirvydas, Thermal analysis of CASTOR RBMK-1500 casks during long-term storage of spent nuclear fuel, Ann. Nucl. Energy 99 (2017) 40–46, https://doi.org/10.1016/j.anucene.2016.09.031.

[17] J. Benavides, G. Jimenez, M. Galbán, M. Lloret, Methodology for thermal analysis of spent nuclear fuel dry cask using CFD codes, Ann. Nucl. Energy 133 (2019) 257–274, https://doi.org/10.1016/j.anucene.2019.05.026.

[18] R. Poškas, V. Šimonis, H. Jouhara, P. Poškas, Modeling of decay heat removal from CONSTOR RBMK-1500 casks during long-term storage of spent nuclear fuel, Energy (Calg.) 170 (2019) 978–985, https://doi.org/10.1016/j.energy.2018.12.217.

[19] J. Benavides, O.C. Garrido, G. Jimenez, L. Cizelj, Thermo-mechanical analysis of a nuclear spent fuel dry cask using CFD results in a FE code, Nucl. Eng. Des. 384 (2021) 111481, https://doi.org/10.1016/j.nucengdes.2021.111481.

[20] E.T. Palmer, B.M. Matthew, Rapid analytic determination of dry cask storage canister, Int. Temp. Transactions. 122 (2020) 63–65. https://www.ans.org/pubs/transactions/article-48179/.

[21] R. Poškas, K. Račkaitis, P. Poškas, H. Jouhara, The numerical analysis of the impact of CASTOR-1500 cask model simplifications on temperature distribution in the cask, Ann. Nucl. Energy 184 (2023) 109688, https://doi.org/10.1016/j.anucene.2023.109688.

[22] R. Poškas, K. Račkaitis, P. Poškas, H. Jouhara, Modelling of the fire impact on CONSTOR RBMK-1500 cask thermal behavior in the open interim storage site, Nucl. Eng. Technol. 55 (2023) 2604–2612, https://doi.org/10.1016/j.net.2023.04.026.

[23] IAEA. Safety Standards Series No. SSR-6 (Rev. 1), Regulations for the Safe Transport of Radioactive Material. Specific Safety Requirements, 2018.

[24] J.Y. Murthy, S.R. Mathur, Finite volume method for radiative heat transfer using unstructured meshes, J. Thermophys. Heat Tran. 12 (1998) 313–321, https://doi.org/10.2514/2.6363.